

A refined empirical stability criterion for nonlinear Schrödinger solitons under spatiotemporal forcing

Franz G. Mertens*

Physikalisches Institut, Universität Bayreuth, D-95440 Bayreuth, Germany

Niurka R. Quintero†

*Departamento de Física Aplicada I, E.U.P., Universidad de Sevilla,
c/ Virgen de África 7, 41011 Sevilla, Spain*

I. V. Barashenkov

Department of Mathematics, University of Cape Town, Rondebosch 7701, South Africa

A. R. Bishop

Los Alamos National Laboratory, Los Alamos, NM 87545, USA

(Dated: February 20, 2018)

We investigate the dynamics of travelling oscillating solitons of the cubic NLS equation under an external spatiotemporal forcing of the form $f(x, t) = a \exp[iK(t)x]$. For the case of time-independent forcing a stability criterion for these solitons, which is based on a collective coordinate theory, was recently conjectured. We show that the proposed criterion has a limited applicability and present a refined criterion which is generally applicable, as confirmed by direct simulations. This includes more general situations where $K(t)$ is harmonic or biharmonic, with or without a damping term in the NLS equation. The refined criterion states that the soliton will be unstable if the “stability curve” $p(v)$, where $p(t)$ and $v(t)$ are the normalized momentum and the velocity of the soliton, has a section with a negative slope. Moreover, for the case of constant K and zero damping we use the collective coordinate solutions to compute a “phase portrait” of the soliton where its dynamics is represented by two-dimensional projections of its trajectories in the four-dimensional space of collective coordinates. We conjecture, and confirm by simulations, that the soliton is unstable if a section of the resulting closed curve on the portrait has a negative sense of rotation.

PACS numbers: 05.45.Yv,

* Franz.Mertens@uni-bayreuth.de

† niurka@us.es

I. INTRODUCTION

The externally driven, nonlinear Schrödinger (NLS) equation arises in many applications, for example charge density waves [1], long Josephson junctions [2], optical fibers [3–5] or plasmas driven by rf fields [6]. We use the NLS in the form

$$iu_t + u_{xx} + 2|u|^2u + \delta u = R[u(x, t); x, t], \quad (1)$$

with the perturbation

$$R = f(x, t) - i\beta u(x, t), \quad (2)$$

where $f(x, t)$ is a direct (external) driving force and the term with β accounts for dissipation. Different forms of the driving force were considered: e.g., ac driving $f = \epsilon \exp(i\omega t)$ [1, 7, 8] or driving by a plane wave $f = \epsilon \exp[i(kx - \omega t)]$ [5, 9]. Moreover, $f = \epsilon \exp[ig(x, t) - i\omega t]$, where g is a function of $x - vt$, was considered, but no localized solutions were discussed [9].

The present paper continues the analysis [10] of the soliton dynamics under the spatiotemporal driving

$$f(x, t) = ae^{iK(t)x}. \quad (3)$$

A discrete version of Eq. (1) was used to model nonlinear optical waveguide arrays, in which discrete cavity solitons can be excited [11]. In that application, δ is the cavity detuning parameter, and $f(x, t)$ is replaced with $f_n(t) = a \exp(i\phi_{in}n)$, where n numbers the resonators and $\phi_{in}(t)$ is the incident angle of the laser pump light. A biharmonic function $\phi_{in}(t)$ was used in order to generate a ratchet effect [12]. In the present paper we also obtain a ratchet effect by using a biharmonic driving (Section V). This is interesting because there are only a few reports on ratchets with nontopological solitons [12–14]; most of the literature concerns ratchets with topological solitons, e.g [15–19].

In Ref. [10], Eq. (1) was simulated using the 1-soliton solution of the unperturbed NLS as the initial condition. The soliton's position, velocity, amplitude and phase served as parameters of the initial condition (IC).

In the case of zero damping and time-independent, spatially periodic driving of the form $f(x) = \exp(iKx)$ the resulting solitons were observed [10] to display periodic oscillations of their positions, velocities, amplitudes and phases. Although the driving force has zero spatial average, the soliton's net motion is *unidirectional*. (This contrasts with the case of

a perturbation $V(x)u$ with periodic $V(x)$, where the soliton performs oscillations about a minimum of $V(x)$ [20]).

A large number of sample points in the parameter space (a, K, δ) were examined by varying the initial amplitude η_0 , with the other initial conditions kept fixed. The initial configuration was seen to evolve into a stable soliton only when η_0 was taken from one of the “stability windows”. For η_0 outside the stability windows, the solitonic initial condition was observed to decay or break into two or more fragments which would subsequently decay [10].

As a first step towards understanding the observed dynamics of solitons, the authors of Ref. [10] proposed an empirical stability criterion based on a collective coordinate (CC) description. The collective coordinates analysis produces a set of coupled nonlinear ODEs for the soliton’s position q , amplitude η , normalized momentum p and phase Φ . An approximate solution of this dynamical system is given by trigonometric functions and can be obtained explicitly, except when the initial condition η_0 is chosen near one of the stability boundaries. In the latter case the collective coordinates equations had to be analysed numerically and their solutions were found to be highly anharmonic.

We have positively tested the predictions of the proposed stability criterion by simulations (numerical solutions of the full NLS Eq. (1)) for many classes of initial conditions. However, the tests are negative, if the initial momentum is too large, i.e. $p_0 > K$ for positive K (or $p_0 < K$ for negative K). In this paper we therefore conjecture a refined stability criterion, which we show makes correct predictions not only for the case $K = \text{constant}$ (with all classes of initial conditions), but also for harmonic and biharmonic $K(t)$. The new criterion is a sufficient condition which states that the soliton will be unstable in simulations, if the “stability curve” $p(v)$ has a branch with negative slope. This curve is obtained as a parametric plot of the *normalized* momentum

$$p = \frac{P(t)}{N(t)}, \quad (4)$$

of the soliton versus its velocity,

$$v = \dot{q}(t). \quad (5)$$

Here $P = 4\eta p$ is the canonical momentum of the soliton, $N = 4\eta$ is the norm which is canonically conjugated to the soliton’s phase $\Phi(t)$, see Section II. In the old criterion [10] the stability curve was defined as $P(v)$. At the end of Section III we present an example

which demonstrates by an analytical calculation that the normalized momentum p , instead of the canonical momentum P , has to be used for the stability criterion.

It is important to emphasize that the soliton's stability or instability is judged not on the basis of the stability of solutions to the collective coordinates equations. (The latter are stable in most cases). The soliton's stability is rather decided on the basis of some of its properties which are captured by the $p(v)$ curve of the corresponding collective coordinates solutions. The proposed empirical criterion reproduces the numerically observed positions of the stability windows to an accuracy of better than 1%, despite the complexity of the stability diagram in the parameter space [10].

The stability criteria for the homogeneous (translation invariant) NLS equation available in the literature are restricted to (a) bright solitons, i.e. solutions decaying to zero at the spatial infinities, with time dependencies of the form $e^{i\Lambda t}$ (and those reducible to this form by a Galileian transformation); (b) traveling dark solitons, i.e. solutions approaching nonzero constant values as $x \rightarrow \pm\infty$. The criteria are insensitive to the particular form of the nonlinearity as long as it is conservative and $U(1)$ -invariant, i.e. as long as the equation does not include any damping or driving terms.

In the case of the bright solitons of the form $u(x, t) = u_s(x)e^{i\Lambda t}$, the Vakhitov-Kolokolov criterion states that if the corresponding energy Hessian has only one negative eigenvalue, then the soliton is stable if $dN/d\Lambda > 0$ and unstable otherwise [21–23]. Here $N = \int |u|^2 dx$; depending on the physical context, N is referred to as the number of particles contained in the soliton or the total power of the optical beam. (See also [24] for the energy-versus-number of particles formulation of this criterion.)

In the case of dark solitons of the form $u(x, t) = u(x - \tilde{V}t)$, with $|u|^2 \rightarrow \rho_0$ as $|x| \rightarrow \infty$, a similar criterion [25–28] involves the (renormalised) field momentum,

$$\tilde{P} = \frac{i}{2} \int (u_x^* u - u_x u^*) \left(1 - \frac{\rho_0}{|u|^2} \right) dx. \quad (6)$$

The dark soliton travelling at the constant velocity \tilde{V} is stable if $d\tilde{P}/d\tilde{V} < 0$ and unstable otherwise.

Some parts of the stability analysis of the travelling dark solitons [27] can be carried over to the case of the travelling solitons of the NLS with a driving term. Namely, one can show [29] that a linearised eigenvalue crosses from the negative to the positive real axis at the value \tilde{V} where $d\tilde{P}/d\tilde{V} = 0$. The sign of the derivative $d\tilde{P}/d\tilde{V}$ required for stability depends

on the type of the soliton; some classes of solitons require $d\tilde{P}/d\tilde{V} < 0$, whereas other classes are stable when $d\tilde{P}/d\tilde{V} > 0$. (An additional complication is the presence of oscillatory instabilities where two eigenvalues collide on the imaginary axis and acquire opposite real parts. The oscillatory instabilities do not affect the sign of $d\tilde{P}/d\tilde{V}$.)

In these analyses, each point of the curve $\tilde{P}(\tilde{V})$ represents a soliton traveling at a particular constant velocity \tilde{V} ; therefore the curve is a characteristic of the whole family of solitons. The values of \tilde{V} where $d\tilde{P}/d\tilde{V} = 0$ break the family into parts with different stability properties. In contrast to this, each oscillatory solution of the collective coordinates equations [10] has its own, individual, $p(v)$ -curve the whole of which is traced periodically in time. The shape of this curve determines whether the corresponding soliton is stable or not.

The present paper has several goals: First, we propose a refined stability criterion. Second, we study the internal structure of the instability regions. We will demonstrate that these regions consist of subregions characterized by instabilities of different types. The existence of the subregions will be predicted by the analysis of the reduced dynamical system and confirmed by direct simulations of the full PDE (Section III). In obtaining the reduced dynamical system we modify the original collective coordinates approach of Ref. [10] (Section II). In addition to producing bounded trajectories (a property essential for the stability analysis), the modified approach provides a much easier derivation of the canonical soliton momentum and the Hamilton function in terms of the canonical variables (Section II).

Third, we demonstrate that a certain “phase portrait” of the soliton on the complex plane can be used as an alternative stability diagnostic (Section III). However, the phase portrait requires the phase of the soliton to be periodic in time. This can be achieved by the above mentioned modification of the original collective coordinates approach [10] in which the phase was *not* periodic, in contrast to the other three collective coordinates.

Finally, we explore the applicability of our refined stability criterion to inhomogeneous forcings of the form $f(x, t) = a \exp(iK(t)x)$ in Eq. (3). We will start with a harmonically varying $K(t)$, with and without the damping term in the right-hand side of (1) (Section IV). After that, in Section V, we will consider a *biharmonic* $K(t)$ with a broken temporal symmetry. (The temporal symmetry breaking will accompany the breaking of the spatial symmetry by the inhomogeneous driving.)

II. MODIFIED COLLECTIVE COORDINATE THEORY

The one-soliton solution of the unperturbed NLS is given by [30]

$$u(x, t) = 2i\eta \operatorname{sech}[2\eta(x - \zeta)]e^{-i(2\xi x + \phi)}, \quad (7)$$

where η and ξ are real parameters ($\eta > 0$); $\zeta = \zeta_0 - 4\xi t$ gives the coordinate of the soliton's center, and $\phi = \phi_0 + (4\xi^2 - 4\eta^2 - \delta)t$ is the soliton's phase. The collective coordinates theory of Ref. [10] assumed that for sufficiently small perturbations R in Eq. (2) the soliton shape and dynamics can be described, approximately, by Eq. (7), where $\eta(t)$, $\xi(t)$, $\zeta(t)$ and $\phi(t)$ are functions of time.

We now show that the following modification of this ansatz [31, 32] provides a considerable improvement of the collective coordinates theory of Ref. [10]:

$$u(x, t) = 2i\eta \operatorname{sech}[2\eta(x - q)]e^{i[p(x-q) - \Phi]}, \quad (8)$$

by setting $-2\xi = p$, $\zeta = q$, and $\phi = \Phi - 2\xi\zeta = \Phi + pq$. Here only the last replacement is essential for the above mentioned improvement of the collective coordinates theory. The four collective coordinates equations of Ref. [10] are replaced with

$$\dot{\eta} = -2\beta\eta - \frac{\pi}{2}a \operatorname{sech}A \cos B, \quad (9)$$

$$\dot{q} = 2p + \frac{\pi^2}{8} \frac{a}{\eta^2} \operatorname{sech}A \tanh A \sin B, \quad (10)$$

$$\dot{p} = -2aA \operatorname{sech}A \cos B, \quad (11)$$

$$\dot{\Phi} + p\dot{q} = p^2 - 4\eta^2 - \delta + \frac{\pi}{2} \frac{aA}{\eta} \operatorname{sech}A \tanh A \sin B, \quad (12)$$

with

$$A(t) = \frac{\pi}{4\eta(t)} [K(t) - p(t)], \quad (13)$$

$$B(t) = \Phi(t) + K(t)q(t). \quad (14)$$

The new formulation has the following advantages

1. Consider the Lagrangian for Eqs. (9)-(12):

$$L = 4\eta\dot{\Phi} + 4\eta p\dot{q} - 4\eta p^2 + \frac{16}{3}\eta^3 + 4\delta\eta - 2\pi a \operatorname{sech}A \sin B. \quad (15)$$

The momentum conjugate to the phase Φ is

$$\frac{\partial L}{\partial \dot{\Phi}} = 4\eta, \quad (16)$$

which is equal to the norm ($\int |u|^2 dx$) of the waveform (8). The momentum conjugate to the soliton's position is

$$\frac{\partial L}{\partial \dot{q}} = 4\eta p. \quad (17)$$

The advantage of the new formulation is that this is equal to the field momentum of the configuration (8)

$$P = \frac{i}{2} \int_{-\infty}^{+\infty} (u_x^* u - u_x u^*) dx, \quad (18)$$

whereas in Ref. [10] the second canonical momentum was defined by $\partial L/\partial \dot{p} = -4\eta q$ which did not have any obvious physical interpretation.

If the dissipative term $-i\beta u$ in (2) has a nonzero coefficient, we have to use the generalised Euler-Lagrange formalism with the dissipation function

$$F = i\beta \int_{-\infty}^{+\infty} (u u_t^* - u^* u_t) dx. \quad (19)$$

Substituting (8) in (19), we obtain

$$F = -8\beta\eta(\dot{\Phi} + p\dot{q}). \quad (20)$$

The generalised Euler-Lagrange equations are

$$\frac{d}{dt} \frac{\partial L}{\partial \dot{\Psi}} - \frac{\partial L}{\partial \Psi} = \frac{\partial F}{\partial \dot{\Psi}}, \quad (21)$$

where Ψ represents each of the four collective coordinates η , q , p , and Φ .

2. Since $P = 4\eta p$ is the canonically conjugate momentum for q , the Legendre transform to the canonical Hamiltonian is easily performed: $H = N\dot{\Phi} + P\dot{q} - L$. This gives

$$H = \frac{1}{N} P^2 - \frac{1}{12} N^3 - \delta N + 2\pi a \operatorname{sech} A \sin B. \quad (22)$$

In Ref. [10] this Hamiltonian could only be obtained via a canonical transformation.

When the forcing $f(x) = ae^{iKx}$ is time-independent and damping $\beta = 0$, the collective coordinates η and p perform periodic oscillations, whereas $q(t)$ and $\Phi(t)$ are given by periodic functions superimposed over linearly growing functions of t . In contrast to this, the variable $\phi = \Phi + pq$ used in Ref. [10] will obviously exhibit oscillations with a (linearly) growing amplitude.

III. TIME-INDEPENDENT, SPATIALLY PERIODIC FORCE

Our approach consists in the numerical solution of the collective coordinates equations (9)-(12) for representative values of the parameters and the initial conditions η_0 , q_0 , p_0 and Φ_0 . Each collective coordinates orbit is then used to compute $p(t)$ and $v(t)$ in Eqs. (4)-(5) and to plot p against v . If some part of this “stability curve” has a negative slope, we predict that the soliton will become unstable in simulations of the PDE (1) starting with the initial condition (8), with the same η_0 , p_0 , q_0 and Φ_0 .

Since the collective coordinates approximation can work only for small perturbations, we choose a small driving amplitude $a = 0.05$ for $f(x) = ae^{iKx}$. We also take $K = 0.1$, which means that the spatial period of the forcing $L = 2\pi/K \gg 1$. We are interested in periodic solutions and therefore we set the damping parameter $\beta = 0$. Damped oscillatory solutions were already considered in Ref. [10].

For $\delta \geq 0$, the $p(v)$ curve predicts only unstable solitons which is confirmed by the simulations. For $\delta < 0$, there are typically several stability regions which grow as $|\delta|$ is increased, while the parameters a and K are fixed [10]. We concentrate here on the simplest case with only one stability and one instability region. Namely, we choose $\delta = -1$, $q_0 = p_0 = \Phi_0 = 0$ for which the soliton solutions are predicted to be stable if $\eta_0 \geq \eta_c^{(1)} = 0.684$ (Fig. 1a) and unstable for $\eta_0 < \eta_c^{(1)}$. This is confirmed by our simulations of the PDE (1) to an accuracy of better than 1% in $\eta_c^{(1)}$.

The range of initial amplitudes η_0 for which solutions of Eqs. (9)-(12) feature a $p(v)$ curve with a descending branch, can be divided into two subintervals, $0 < \eta_0 < \eta_c^{(2)}$ and $\eta_c^{(2)} < \eta_0 < \eta_c^{(1)}$, where $\eta_c^{(2)} = 0.288$. In the upper subinterval, $(\eta_c^{(2)}, \eta_c^{(1)})$, the curve $p(v)$ exhibits two long branches, one with a positive and the other with a negative slope (Fig. 1b). In the lower subinterval, the positive-slope branch is short and very steep (Fig. 1c). The difference in the shape of the stability curves suggests different types of instability in the two subregions; however, in which way the instabilities are different cannot be deduced from the $p(v)$ curve alone. To gain further insight into this difference, we plot a phase portrait for the dynamical system (9)-(12). The vertical and horizontal axes in the portrait are chosen so that they admit a clear interpretation in terms of the full PDE, Eq. (1). To this end, we

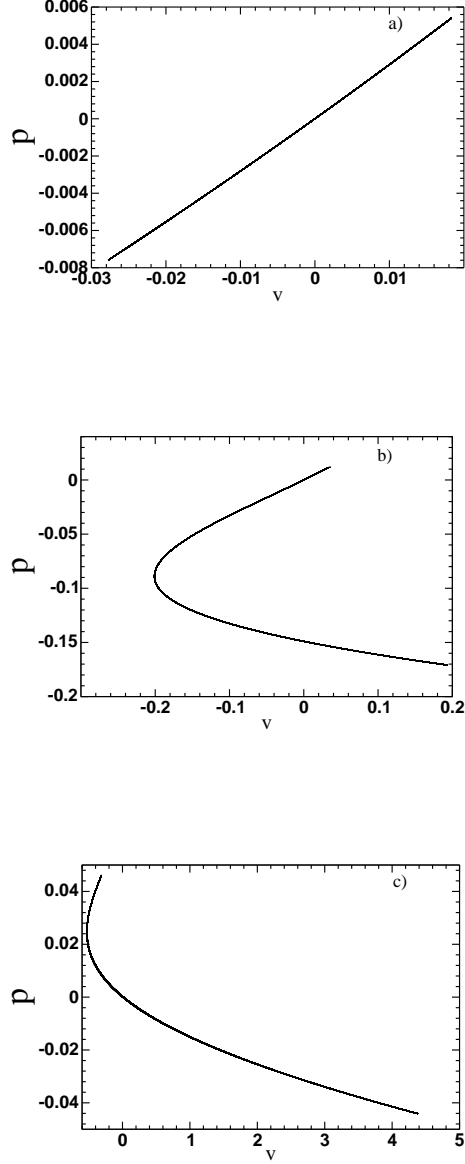


FIG. 1. Stability curve $p(v)$ corresponding to $a = 0.05$, $K = 0.1$, $\delta = -1$ and $\beta = 0$. The initial conditions for the Eqs. (9)-(12) were $q_0 = p_0 = \Phi_0 = 0$ and a) $\eta_0 = 0.8$, b) $\eta_0 = 0.65$, c) $\eta_0 = 0.1$. The integration time $t_f = 1000$.

first transform to the frame of reference moving with the velocity V_f :

$$u(x, t) = \Psi(X, t)e^{iKx}, \quad X = x - V_f t, \quad (23)$$

where $V_f = 2K$. Eq. (1) is taken to be an NLS driven by a space-time independent external force:

$$i\Psi_t + \Psi_{XX} + 2|\Psi|^2\Psi + (\delta - K^2)\Psi = a. \quad (24)$$

(This equation was previously studied in a different context [7, 8, 33, 34] and two static soliton solutions were obtained explicitly [34]. Unlike [7, 8, 33, 34], we focus here on moving solitons of Eq. (24).)

Under the transformation (23), the collective coordinates ansatz (8) becomes

$$\Psi(X, t) = 2i\eta \operatorname{sech}[2\eta(X + V_f t - q)]e^{-i[(K-p)(X+V_f t)+pq+\Phi]}. \quad (25)$$

The $\eta(t)$ and $p(t)$ components of the oscillatory solutions of (9)-(12) are periodic with period T , whereas q and Φ are of the form $q(t) = \bar{v}t + q^{(p)}(t)$, $\Phi(t) = -\alpha t + \Phi^{(p)}(t)$, where $q^{(p)}(t)$ and $\Phi^{(p)}(t)$ are T -periodic functions and α is a constant [10]. The corresponding soliton (8), (25) has the mean velocity \bar{v} in the original frame of reference, and $\bar{v} - V_f$ in the moving frame.

At the point $x = \bar{v}t$ [or, equivalently, at $X = (\bar{v} - V_f)t$], the function (25) has the following time dependence:

$$\Psi = 2i\eta \operatorname{sech}[2\eta(\bar{v}t - q)]e^{-i[K\bar{v}t - p(\bar{v}t - q) + \Phi]}. \quad (26)$$

The function (26) is a collective coordinates counterpart of the Ψ field at the centre of the soliton solution of Eq. (24). Comparing Eq. (26) to the function $\Psi(X, t)|_{X=\bar{v}t-V_f t}$ obtained in the direct numerical simulations of the full PDE (1), one can assess the validity and accuracy of the collective coordinates approximation. For this reason, we choose the complex function (26) as a representative of the four-dimensional dynamics, and plot its real versus imaginary part to generate the corresponding phase portrait. The soliton dynamics is described by the resulting orbits of the phase portrait.

One can readily verify that these orbits are closed. Indeed, the modulus of the function (26) is periodic with period T . Therefore, to demonstrate the closure, one just needs to show that the argument of Ψ changes by an integer multiple of 2π over the period. We have $\arg \Psi = (\alpha - K\bar{v})t - p^{(p)}q^{(p)} - \Phi^{(p)}$, where the last two terms are T -periodic. As for the first term, the constants \bar{v} and α are found as the coefficients of the linearly-growing components of $q(t)$ and $\Phi(t)$, respectively. The numerical solution of Eqs. (9)-(12) verifies that $\alpha - K\bar{v} = 2\pi/T$ in the stability range $\eta_0 \geq \eta_c^{(1)}$, that $\alpha - K\bar{v} = -2\pi/T$ in the lower instability subinterval $0 < \eta_0 < \eta_c^{(2)}$, and $K\bar{v} - \alpha = 0$ in the upper instability subinterval $\eta_c^{(2)} < \eta_0 < \eta_c^{(1)}$. These relations between \bar{v} and α hold to a numerical accuracy of $O(10^{-5})$.

Trajectories resulting from initial conditions in the interval $\eta_0 > \eta_c^{(1)}$ are ellipses, with a positive sense of rotation (Fig. 2). The ellipses enclose a stable and an unstable fixed point

on the real axis at about $+1$ and -1 , respectively. (For the definition and calculation of these points see Appendix A). Fig. 3a compares the soliton amplitude $\eta(t)$ from collective coordinates theory to the amplitude measured in the direct simulations of Eq. (1).

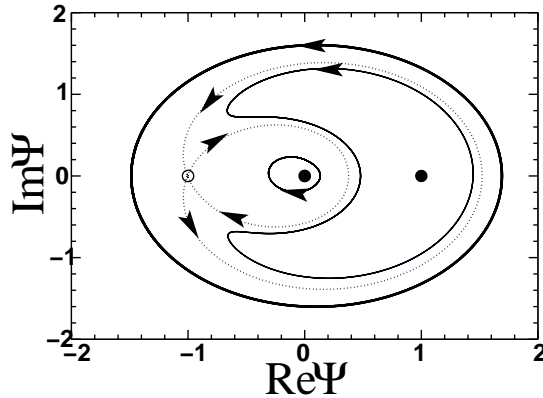


FIG. 2. The phase portrait of the system (9)-(12) with a , K , δ and β as in Fig. (1). Shown is $\text{Im}\Psi(X = \bar{v}t - V_f t, t)$ versus $\text{Re}\Psi(X = \bar{v}t - V_f t, t)$. The large ellipse corresponds to $\eta_0 = 0.8$, the horseshoe to $\eta_0 = 0.65$ and the small ellipse to $\eta_0 = 0.1$. Other initial conditions are as in Fig. (1). The separatrix is shown by the dotted curve. The filled and open circles are stable and unstable fixed points, respectively.

For the upper instability subinterval $\eta_c^{(2)} < \eta_0 < \eta_c^{(1)}$ the phase trajectory is a horseshoe (Fig. 2). This curve consists of an outer part with a positive sense of rotation and an inner part with a *negative* sense of rotation relative to the origin. The two parts are correlated with the two branches with positive and negative slopes, respectively, of the $p(v)$ -curve in Fig. 1b. The soliton instability is seen in the simulation result in Fig. 3b. Note that the first harmonic vanishes after about 30 time units, while the second harmonic persists. Eventually the soliton decays: the amplitude approaches zero while the width tends to infinity.

For the lower instability interval $0 < \eta_0 < \eta_c^{(2)}$ the situation is quite different, both in the collective coordinates theory and in the simulations: The phase portrait features an ellipse, but with the *negative* sense of rotation (Fig. 2). Moreover, the ellipse is much smaller than the one arising in the stability region so that it encloses only one fixed point. This fits with the simulations in which the soliton remains metastable for a relatively long time, exhibiting

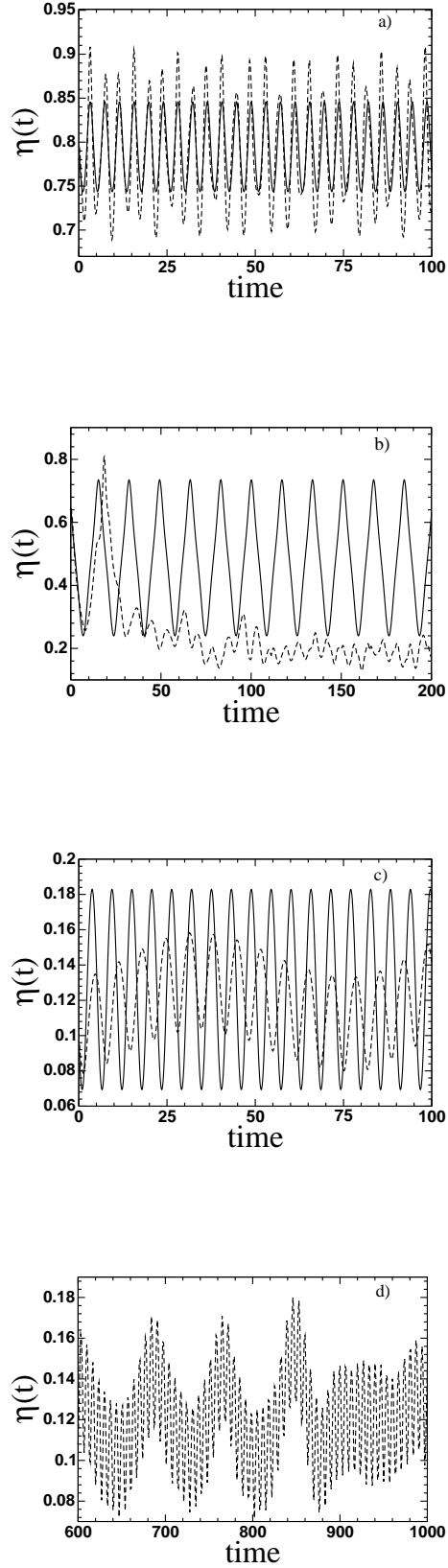


FIG. 3. Soliton amplitude $\eta(t)$ from the collective coordinates theory (solid lines) and from the simulations (dashed lines). The parameters and the initial conditions are the same as in Fig. 1. a) $\eta_0 = 0.8$, b) $\eta_0 = 0.65$, c) $\eta_0 = 0.1$ (shown are results for early times $0 \leq t \leq 100$); d) $\eta_0 = 0.1$ (shown are simulation results for late times $600 \leq t \leq 1000$.)

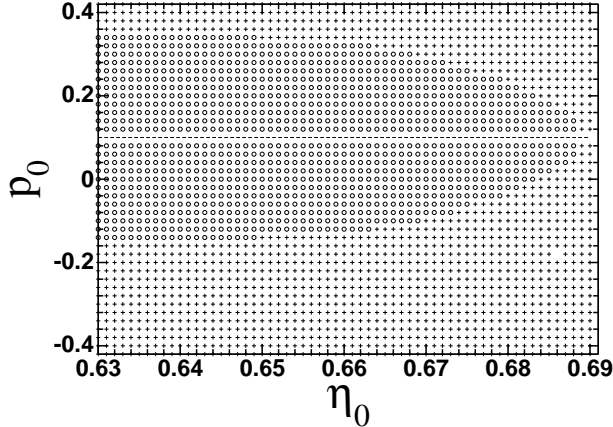


FIG. 4. Stability diagram near $\eta_c^{(1)} = 0.684$, with $q_0 = \Phi_0 = 0$. Parameters: $a = 0.05$, $K = 0.1$, $\delta = -1$, $\beta = 0$. Circles: unstable soliton. Plus: stable soliton. Dashed line: for $p_0 = K$, the $p(v)$ curve is a point.

a periodic modulation of the oscillation amplitude (Fig. 3c), but then the instability sets in (Fig. 3d).

So far we have varied η_0 , with $p_0 = q_0 = \Phi_0 = 0$ kept fixed. We now consider the stability diagram in the η_0 - p_0 plane near the critical value $\eta_c^{(1)}$, which separates the stability interval from the upper instability interval (above). Fig. 4 shows that a finite value of the normalized momentum p_0 stabilizes the soliton and therefore the stability region is enlarged. The curve which separates stability and instability regions is roughly a parabola.

Finally we would like to emphasize the crucial importance of using the *normalized* momentum p in the stability analysis —rather than the canonical momentum P (as was proposed in [10]). We have established that the empirical stability criterion suggested in [10] disagrees with the results of numerical simulations when the initial normalized momentum is too large, i.e. $p_0 > K$ (for positive K). Let, for instance, the parameters of the equation take the same values as in Fig. 1 ($a = 0.05$, $K = 0.1$, $\delta = -1$ and $\beta = 0$), and take the same initial conditions as for the stable stationary solution in the Appendix ($\eta_0 = 0.5\sqrt{K^2 - \delta}$, $\Phi_0 = \pi/2$, $q_0 = 0$), except that this time $p_0 = K + d$, where $0 < d < 0.2$. In this case the numerical solutions of the collective coordinates equations can be represented in a very good approximation by $p(t) = p_0 + a_p(1 - \cos \Omega t)$ and $v(t) = v_0 + a_v(1 - \cos \Omega t)$, where p_0 , v_0 , a_p , $a_v > 0$. Thus $p(v)$ is a straight line with slope $a_p/a_v > 0$. This predicts stability, the same as the orbit in the phase portrait which is a small ellipse with positive sense of rotation

around the stable fixed point at about +1 on the real axis. The stability is confirmed by simulations. However, when the momentum $P = 4\eta p$ is used the situation is different. $\eta(t)$ can be expressed via $p(t)$ by using the exact relation $\eta = \eta_0(p_0 - K)/(p - K)$ ($p \neq K$), which is obtained from Eqs. (9) and (11) where one integration has been carried out. Finally, $p(v)$ from above is inserted and one can see that P decreases when v increases and viceversa. Thus the slope $dP/dv < 0$ predicts instability which disagrees with the simulations.

IV. HARMONIC $K(t)$

As stated in the Introduction, one of the aims of this paper is to verify whether the stability criterion $p'(v) > 0$ remains applicable to time-dependent forces of the form $f(x, t) = ae^{iK(t)x}$. In this section we consider the case of a harmonically modulated forcing wavenumber:

$$K(t) = k \sin(\omega t + \theta), \quad (27)$$

first without a damping term in the NLS ($\beta = 0$), then with the damping ($\beta > 0$).

We choose the same parameters as in Section III: $a = 0.05$, $k = -0.1$ which implies $|K| \ll 1$. In order to be in the adiabatic regime we choose a small modulation frequency $\omega = 0.02$. Finally, we let $\theta = 0$ and choose initial conditions $q_0 = p_0 = 0$, $\eta_0 = 1$, and $\Phi_0 = \pi/2$.

The numerical solutions of the collective coordinates equations (9)-(12) exhibit oscillations with three very different frequencies in their spectrum. This is most explicit in the behaviour of $q(t)$ (Fig. 5 a,b). First, there are intrinsic oscillations with the frequency ω_i ; these have a period T_i of the order of 10, similarly to the oscillations in the case of the constant K discussed in the previous section. Second, there are oscillations with the driving frequency ω whose period $T_d = 2\pi/\omega \approx 314$. Finally, there are oscillations with a very low frequency ω_l and very long period $T_l \approx 8000$ (Fig. 5b). The resulting stability curve $p(v)$ exhibits many small loops which have a short section with a negative slope. An example is given in Fig. 5c. (For clarity the curve is plotted only over a short time interval). The negative slope predicts instability; this is confirmed by our simulations of the full PDE.

Stable solitons can be obtained by changing η_0 in such a way that the loops do not arise. This is achieved by suppressing the intrinsic oscillations, since their period $T_i \approx 10$ is of the

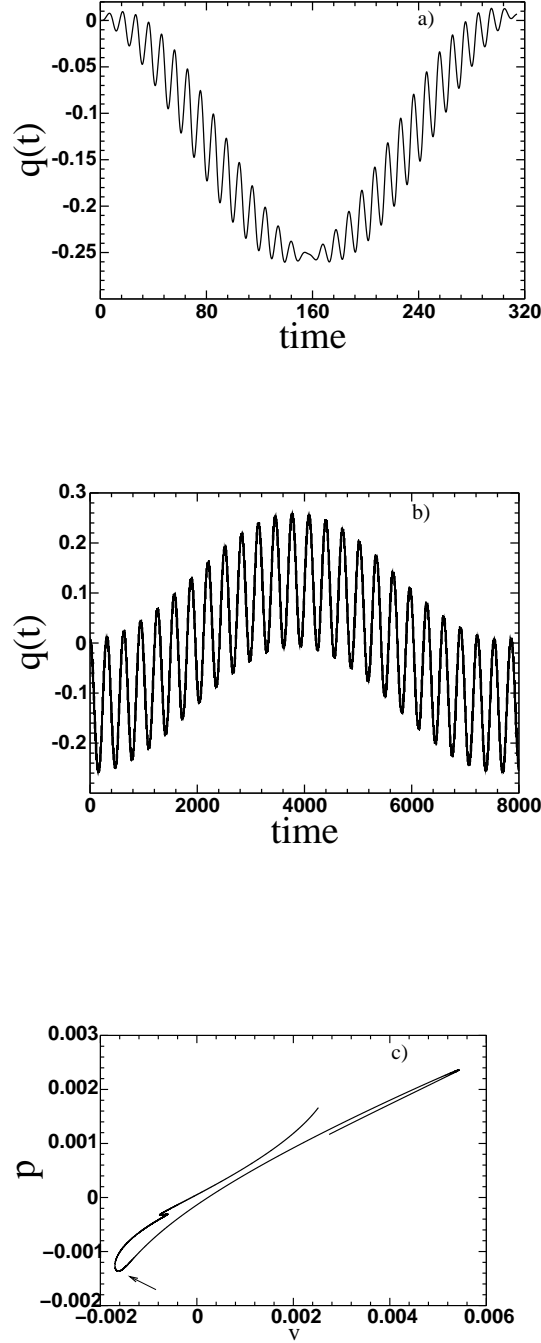


FIG. 5. Collective coordinates results for harmonic $K(t)$, no damping. $a = 0.05$, $k = -0.1$, $\omega = 0.02$, $\theta = 0$, $\delta = -3$, $\beta = 0$, $q_0 = p_0 = 0$, $\Phi_0 = \pi/2$, $\eta_0 = 1$. a) $q(t)$ exhibits ω_i -oscillations modulated by the frequency ω . Shown is the interval $0 \leq t \leq T_d = 2\pi/\omega$. b) $q(t)$ exhibits ω -oscillations modulated by the frequency $\omega_l = 2\pi/T_l$. Here $0 \leq t \leq 8000$. c) Stability curve $p(v)$ for $T_d/2 - 5 \leq t \leq T_d/2 + 10$. The arrow points to the section of the curve with a negative slope loop.

same order as the time scale of the loops, see Fig. 5c. The intrinsic oscillations disappear when we choose $\eta_0 = \sqrt{-\delta}/2$ (Fig. 6a,b). In this case $\eta(t)$ performs very small oscillations around η_0 and the two dominant terms on the r.h.s. of Eq. (12), namely $-4\eta_0^2$ and $-\delta$, cancel each other. Fig. 6c demonstrates that the small loops have indeed disappeared.

The resolution of Fig. 6c does not allow verification of whether there are sections with negative slope near the turning points of the stability curve. We now show that there cannot be any, as the curve develops cusps at the turning points. Consider the region around one of the maxima (or minima) of the ω -oscillations of the collective coordinates (Fig. 6a). The functions $q(t)$, $\eta(t)$ etc. are *not* symmetric with respect to t_m (position of the extremum) due to the existence of the very slow ω_l -oscillations. The same holds for p ; hence

$$p(t) = \begin{cases} p_m - C_l(t - t_m)^2 & \text{for } t \leq t_m \\ p_m - C_r(t - t_m)^2 & \text{for } t \geq t_m \end{cases} \quad (28)$$

with $C_l \neq C_r$. For the velocity $v(t) = \dot{q}(t)$ the asymmetry is negligible, compared to the asymmetry of $p(t)$, because the time derivative \dot{q} contains a factor $\omega_l \ll 1$. Thus $v(t) = v_m - b(t - t_m)^2$ for both $t \leq t_m$ and $t \geq t_m$. Eliminating t we obtain $p = p_m - C_l(v_m - v)/b$ as v increases up to its maximal value v_m , and $v = v_m - C_r(v_m - v)/b$ as v decreases from v_m . Thus the stability curve $p(v)$ has a cusp with two different (but positive) slopes C_l/b and C_r/b at the turning point $v = v_m$. The absence of segments of the curve with $dp/dv < 0$ predicts stability for the soliton. This is confirmed by the simulations of the PDE (1).

When the damping term $-i\beta u$ is included in the r.h.s. of the NLS equation (1), the collective coordinates dynamics simplifies. Namely, both the intrinsic oscillations and the low-frequency oscillations are damped out from solutions of the collective coordinates equations after a transient time $t_{tr} = 1/\beta$. After this transient, all collective coordinates oscillations become locked to the driving frequency ω . The stability curve in this case consists of two nearly-straight lines which form sharp cusps at both ends (Fig. 7a). Thus there are no sections with a negative slope and the soliton is predicted to be stable. This is confirmed by the simulations of the PDE. For long times ($t \gg t_{tr}$) the average soliton velocity \bar{v} slowly approaches zero (Fig. 7b); this behaviour is independent of the initial conditions. Thus there is no unidirectional motion of the soliton for long times; the reason will be established in the next section.

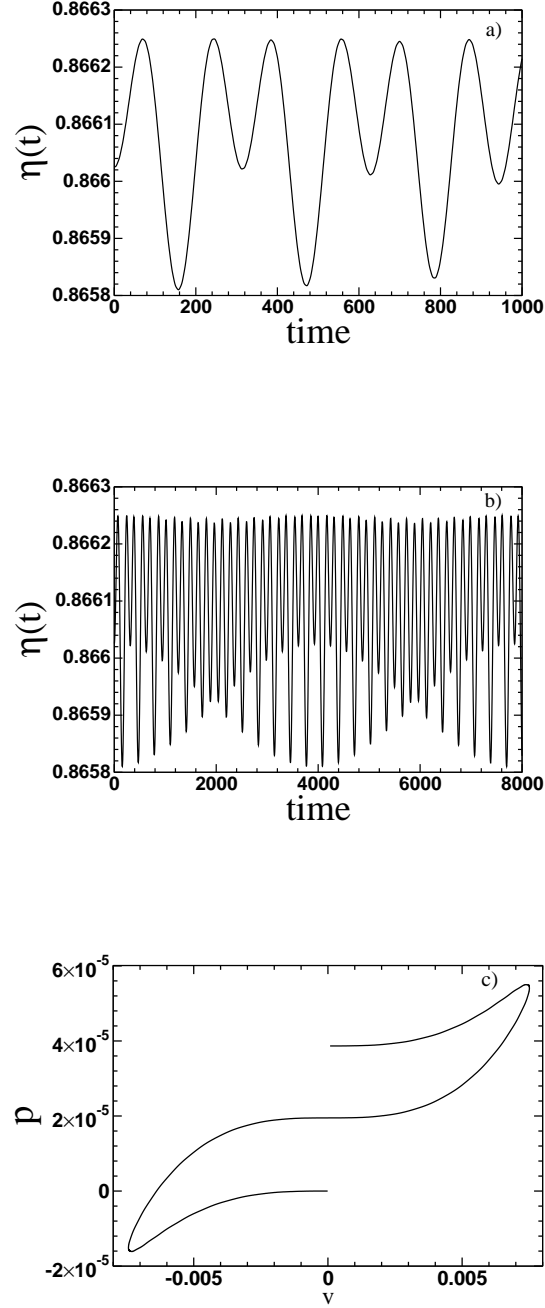


FIG. 6. Collective coordinates results for harmonic $K(t)$, no damping. Same parameters and initial conditions as in Fig. 5, but $\eta_0 = \sqrt{-\delta}/2$. (For this choice the intrinsic ω_i -oscillations vanish.) a) The amplitude $\eta(t)$ exhibits no ω_i -oscillations, only ω -oscillations modulated by ω_l -oscillations which are hardly visible for $0 \leq t \leq 1000$. b) For $\eta(t)$ for $0 \leq t \leq 8000$ both ω - and ω_l -oscillations are visible. c) Stability curve for $0 \leq t \leq T_d$.

As β is decreased, the stability curve becomes wider and the decay of \bar{v} to zero faster.

On the contrary, as β is increased, the stability curve becomes narrower, and \bar{v} decreases to zero more slowly. However, for β above a critical value β_c ($\beta_c \approx 0.035$ for the parameters of Fig. 7) the collective coordinates solutions become unstable. Direct simulations also confirm the soliton's instability.

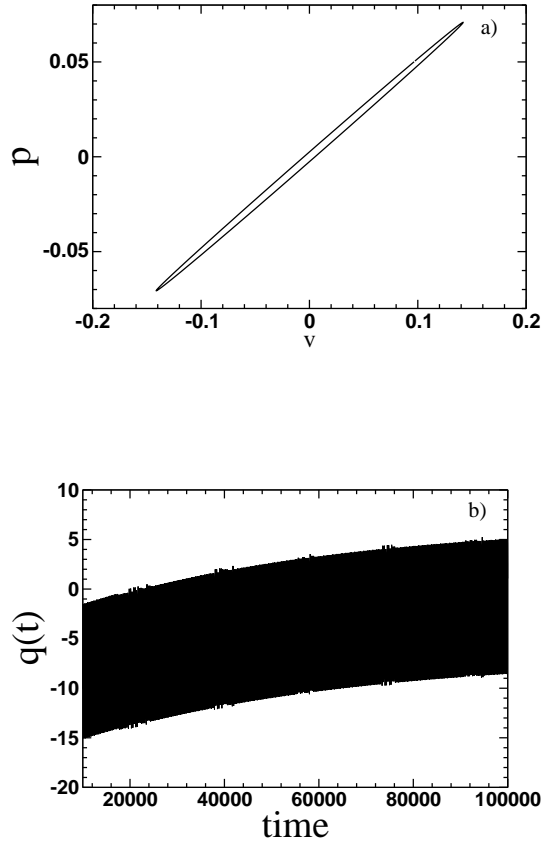


FIG. 7. Collective coordinates results for harmonic $K(t)$, nonzero damping. Same data as in Fig. 6, but $\eta_0 = 0.866 \approx \sqrt{-\delta}/2$, $\beta = 0.01$. a) stability curve $p(v)$ for $3T_d \leq t \leq 4T_d$. b) $q(t)$ for $10000 \leq t \leq 100000$.

V. BIHARMONIC DRIVING: RATCHETS

The simplest ratchet models consider a point-like particle in a periodic potential driven by an AC force $f(t)$. Under certain conditions related to the breaking of symmetries, unidirectional motion of the particle can take place despite the applied force having zero temporal average [35–39]. Particle ratchets were generalized to nonlinear field theoretic systems, in

which particles are replaced by solitons [40–46]. In particular, solitons in nonlinear Klein-Gordon systems can move on the average in one direction, if either a temporal or a spatial symmetry is broken.

A temporal symmetry, namely a time-shift symmetry, is broken by a biharmonic force [47, 48]. In this case the mechanism of the ratchet effect was clarified by a collective coordinates theory employing the soliton position and width as collective coordinates [15, 16, 49]. Due to the coupling between the translational and internal degrees of freedom, energy is pumped nonuniformly into the system, generating a unidirectional motion. The breaking of the time-shift symmetry gives rise to a resonance mechanism that is present whenever the soliton oscillation spectrum comprises at least one of the frequency components of the driving force.

In this section we investigate whether the NLS solitons show a behavior similar to the Klein-Gordon kinks. This is particularly interesting since the NLS solitons are non-topological, whereas the vast majority of reports on soliton ratchets have so far focussed on topological solitons.

We consider the NLS (1) where the perturbation

$$R = f(x, t) - i\beta u, \quad (29)$$

has the form

$$f(x, t) = a_1 e^{iK_1(t)x} + a_2 e^{iK_2(t)x}, \quad (30)$$

with

$$K_1 = k_1 \sin(\omega t), \quad K_2 = k_2 \sin(2\omega t + \theta). \quad (31)$$

Consider first the single-harmonic case: $a_2 = 0$. When $t \gg t_{tr} = 1/\beta$, the soliton oscillations are locked to the driving frequency ω and are independent of the initial conditions (see Section IV). Thus there exists a global solitonic attractor.

We now perform a symmetry analysis [12, 48]. The perturbed NLS is invariant under the symmetry operation

$$\mathcal{S} : t \mapsto t + T/2, \quad x \mapsto -x. \quad (32)$$

At the same time, the transformation \mathcal{S} changes the sign of the soliton velocity $v(t) = \dot{X}(t)$.

The soliton position is defined by

$$X(t) = \frac{\int_{-\infty}^{+\infty} dx x \rho(x, t)}{\int_{-\infty}^{+\infty} dx \rho(x, t)} \quad (33)$$

with

$$\rho(x, t) = ||u(x, t)|^2 - |u_{bg}(x, t)|^2|. \quad (34)$$

Here $u_{bg}(x, t) = a_{bg}(t) \exp(iK_1x)$ is the background field to which the soliton decays as $|x| \rightarrow \infty$ [10, 12]. When $|u(x, t)|^2$ from the simulations is plotted, the soliton sits on a shelf with homogeneous intensity $|a_{bg}(t)|^2$. The shelf has little influence on the soliton dynamics [10]; this is why the collective coordinates theory is in a good agreement with simulations, despite ignoring the presence of the background.

Since the attractor is global, the transformation \mathcal{S} maps it onto itself. This implies that the average velocity on the attractor is zero. The soliton performs periodic oscillations about its equilibrium position which are reproduced by the collective coordinates theory (Fig. 7b).

In order to construct a solitonic ratchet, i.e. obtain a stable soliton with $\bar{v} \neq 0$, it is necessary to break the invariance under the operation \mathcal{S} . The simplest way to do this is to employ the *biharmonic* driving in Eq. (30) with $a_1 \neq 0$ and $a_2 \neq 0$. The collective coordinates equations (9)-(12) can easily be extended to the case of the forcing function f including two terms. In particular, Eq. (9) is replaced with

$$\dot{\eta} = -2\beta\eta - \sum_{i=1}^2 a_i \frac{\pi}{2} \operatorname{sech} A_i \cos B_i, \quad (35)$$

where

$$A_i = \frac{\pi}{4\eta(t)} [K_i(t) - p(t)], \quad (36)$$

$$B_i = \Phi(t) + K_i(t)q(t), \quad (37)$$

while the K_i are as in Eqs. (31). The collective coordinates equations for \dot{q} , \dot{p} and $\dot{\Phi}$ are modified in a similar way.

Since the collective coordinates description is accurate only for small perturbations, we take small driving amplitudes $a_1 = a_2 = 0.05$. We choose a very small driving frequency $\omega = 0.002$ in order to remain in the adiabatic regime. If the damping coefficient β is chosen too large, the soliton amplitude η quickly relaxes to zero while $q(t)$ and $\Phi(t)$ rapidly go to infinity. For example, for the parameters $\delta = -3$, $k_1 = k_2 = k = 0.001$, $\theta = 0$ and the IC $\eta_0 = 1$, $q_0 = p_0 = 0$, $\Phi_0 = \pi/2$, this instability occurs when $\beta > 0.065$. On the other hand, if β is chosen too small (e.g., $\beta = 0.01$), the average soliton velocity grows without bound over sufficiently long integration times ($t_f \sim 10^5$). Thus we can expect a stable ratchet effect

only for intermediate values of β , for instance $\beta = 0.04$. As we find that $\bar{v} \sim k$, a larger ratchet effect can be obtained by increasing k . However, when k exceeds a certain critical value k_c , the average velocity starts to grow slowly with time. (For the chosen parameter values, $k_c = 0.002$).

Using the parameter values and initial conditions for which the collective coordinates equations exhibit stable solutions we perform direct simulations of Eq. (1). Our aim is to test whether an initial waveform (8) will evolve into a stable solitary wave over the time $t_{tr} = 1/\beta$. However, it turns out that the initial structure evolves rapidly immediately after the start of the simulation and quickly decays to zero.

In order to obtain stable solitary waves we need to improve the initial conditions. This can be achieved by setting the initial conditions equal to the mean values about which the collective coordinates oscillate, once the transients have elapsed. These mean values can be obtained from an approximate analytical solution of the collective coordinates equations: We let

$$\begin{aligned} q &= \bar{v}t + C_q, \\ p &= \bar{p} + C_p, \\ \eta &= \bar{\eta} + C_\eta, \\ \Phi &= \bar{\Phi} + C_\Phi, \end{aligned} \tag{38}$$

where C_x are oscillations with amplitude a_x and zero mean. We choose $\omega = O(10^{-3})$, and $k_1 = k_2 = k = O(10^{-3})$. The other parameters $(\delta, a_1, a_2, \beta)$ do not have to be small for the following perturbation analysis and can therefore be chosen in $O(1)$. Substituting in the collective coordinates equations we retain only the leading terms in the perturbation series. This gives

$$\bar{p} = 0, \quad p = \frac{a_1 K_1(t) + a_2 K_2(t)}{(a_1 + a_2)} = O(10^{-3}), \tag{39}$$

$$\bar{\eta} = \frac{1}{2}\sqrt{-\delta}, \quad a_\eta = O(10^{-6}), \tag{40}$$

$$\bar{\Phi} = \arccos\left(\frac{-4\beta\bar{\eta}}{\pi(a_1 + a_2)}\right), \quad a_\Phi = O(10^{-3}), \tag{41}$$

$$q = \bar{v}t + \frac{k}{\omega} \frac{2a_1}{a_1 + a_2} (1 - \cos(\omega t)) + \frac{k}{2\omega} \frac{2a_2}{a_1 + a_2} \tag{42}$$

$$\times (1 - \cos(2\omega t + \theta)), \quad \bar{v} = O(10^{-6}). \tag{43}$$

Eqs. (39)-(42) are in very good agreement with the numerical solution of the collective coordinates equations. We note that the constants \bar{p} , $\bar{\eta}$ and $\bar{\Phi}$ do not depend on the relative phase θ , but the variable components of $q(t)$ and $p(t)$ do.

The improved initial conditions are now: $p_0 = \bar{p} = 0$, $\eta_0 = \bar{\eta}$, $\Phi_0 = \bar{\Phi}$, $q_0 = 0$. After a transient time the numerical trajectory settles to the solution (39)-(42). This yields $v(t) = \dot{q} = 2p$ and thus $p(v) = \frac{1}{2}v$ is a straight line with positive slope. Our stability criterion predicts the stability of the soliton and simulations of the PDE confirm this (Fig. 8a,b). As \bar{v} is very small, the ratchet effect is not visible on the time scale of Fig. 8a,b, but can be observed over longer simulation times $t_f \approx 30T_d$ (Fig. 8c). The soliton collective coordinates amplitude $\eta(t)$ oscillates about 0.866025 in the interval $[0.866024, 0.866026]$, in agreement with Eq. (40). In the simulations, $\eta(t)$ oscillates about 0.87363 in $[0.87305, 0.87390]$.

The ratchet effect is also observed for higher driving frequencies (e.g., $\omega = 0.01$ and 0.02). However, the average velocity \bar{v} decreases in proportion to $1/\omega$, similar to the last two terms in Eq. (42)). It is important to emphasize here that we only succeeded in determining initial conditions for a stable soliton thanks to the availability of the explicit solution of the collective coordinates equations and our stability criterion. It would be very difficult to identify the corresponding small basin of attraction via numerical simulations of the PDE.

Finally, we discuss the dependence of the average velocity \bar{v} on the relative phase θ in the biharmonic driving force (31). As expected for a ratchet system with biharmonic driving [48, 49], $\bar{v}(\theta)$ is sinusoidal with the period 2π . It attains its maximum value near $\theta = 0$ and its small negative minimum value near $\theta = \pi$. The size and shape of the basin of attraction around $(\bar{\eta}, \bar{\Phi})$ also depend strongly on θ ; this effect will be examined in a future work.

VI. SUMMARY

We have formulated a refined empirical stability criterion for the driven NLS solitons. Unlike stability criteria available in the literature, the new criterion is based on a Collective Coordinate (CC) description. Solving (analytically or numerically) evolution equations for the four collective coordinates, we use the resulting trajectories to evaluate the normalized soliton momentum $p(t)$ and the soliton velocity $v(t)$. These give a parametric “*stability curve*”, $p(v)$.

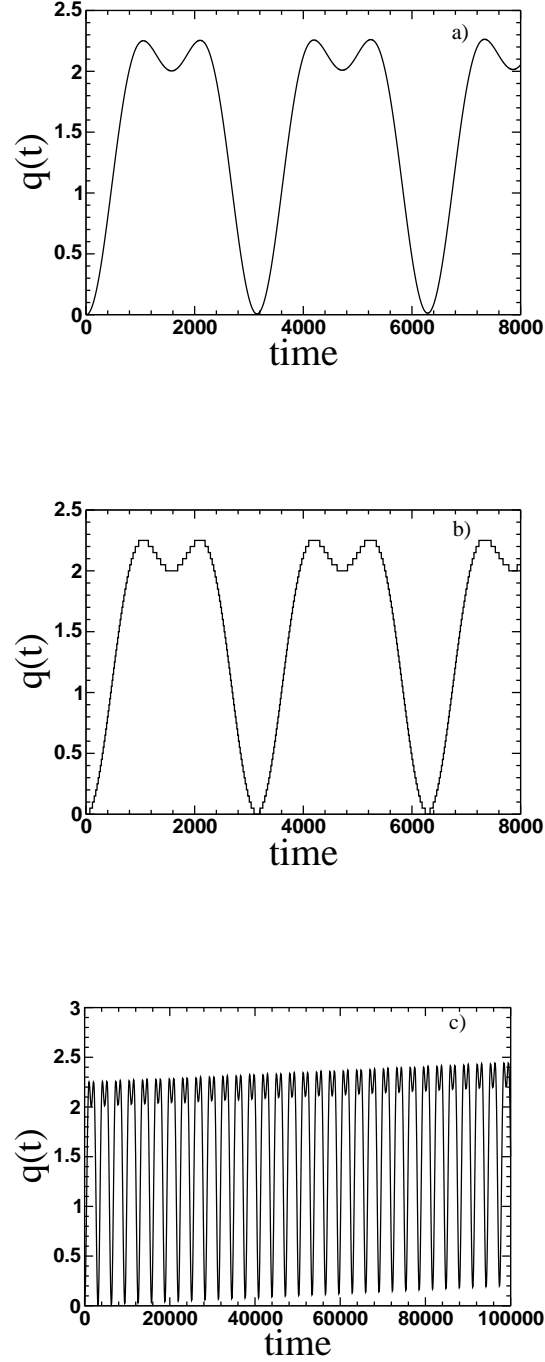


FIG. 8. Soliton position $q(t)$: (a) from the collective coordinates theory, (b) from simulations, (c) the ratchet effect in the collective coordinates theory visible over long times ($t_f \approx 30$ periods). Parameters: $a_1 = a_2 = a = 0.05$, $k_1 = k_2 = k = 0.002$, $\delta = -3$, $\omega = 0.002$, $\theta = 0$, $\beta = 0.08$, with initial conditions $\eta_0 = \bar{\eta}$, $q_0 = p_0 = 0$, $\Phi_0 = \bar{\Phi}$.

Whenever the curve $p(v)$ has a section with a negative slope ($dp/dv < 0$), we observe the

instability of the soliton in direct numerical simulations. We therefore conjecture that the availability of a section with a negative slope is a sufficient condition for the instability of the soliton. We do not have a mathematical proof of this conjectured criterion; however we have verified it in a variety of situations using constant, harmonic and biharmonic functions $K(t)$, with or without the damping term.

Establishing a theoretical justification of this conjecture is a subject of future work, first for the cases of $K(t)$ which we have considered in this paper, then for a general function $K(t)$. One of the foreseen difficulties is related to the fact that the soliton solution of the driven NLS does not vanish as $x \rightarrow \pm\infty$, because the perturbation $f(x, t) = a \exp[iK(t)x]$ does not decay to zero in these limits. On the other hand, our collective coordinates theory is based on a soliton ansatz which vanishes as $x \rightarrow \pm\infty$.

For the case of constant K and zero damping, all collective coordinates perform periodic motions. This allowed us to compute a phase portrait which consists of closed orbits on a complex plane. The soliton evolution is described by motion along one of these orbits. We observe that the sense of rotation of the orbit is correlated with the stability/instability of the soliton (determined in simulations of the full PDE). Namely,

1. If the orbit is an ellipse with a positive sense of rotation, the soliton is stable.
2. If the orbit is a horseshoe where the inner part has negative and the outer part positive sense of rotation, the soliton is unstable and desintegrates very quickly.
3. If the orbit is an ellipse with a negative sense of rotation, the soliton remains metastable for a relatively long time but eventually desintegrates.

An interesting question is whether our collective coordinate approach and our stability criteria can also be applied to NLS equations with a more general form of the nonlinearity. Work is in progress regarding the case of a nonlinearity with arbitrary power, $(u^*u)^\kappa$, where $\kappa = 1$ corresponds to the NLS of this paper. The unperturbed NLS has stable solitons for $0 < \kappa < 2$ and it will be interesting to determine how the stability of the solitons is affected by the perturbation $f(x, t)$.

VII. ACKNOWLEDGMENTS

F.G.M. acknowledges the hospitality of the Mathematical Institute of the University of Seville (IMUS) and of the Theoretical Division and Center for Nonlinear Studies at the Los Alamos National Laboratory. Work at Los Alamos was supported by USDOE. F.G.M. acknowledges financial supports by the Plan Propio of the University of Seville and by Junta de Andalucía under the grant IAC09-III-6399. N.R.Q. acknowledges financial support by the DAAD under the grant A/08/04067, by the Ministerio de Educación y Ciencia (MEC, Spain) through FIS2008-02380/FIS, and by Junta de Andalucía under the projects FQM207, FQM-00481, P06-FQM-01735 and P09-FQM-4643.

VIII. APPENDIX A: FIXED POINTS OF THE PHASE PORTRAIT

For the case of the time-independent force $f(x) = ae^{iKx}$ and zero damping, we adopt the following ansatz for stationary solutions of the collective coordinates equations:

$$q(t) = v_s t, \quad \eta(t) = \eta_s, \quad p(t) = p_s, \quad \Phi(t) = \Phi_s - \alpha_s t. \quad (44)$$

Eq. (9) yields $\cos B \equiv 0$ which results in

$$Kv_s = \alpha_s, \quad \Phi_s^\pm = \pm \frac{\pi}{2}, \quad \sin B = \pm 1. \quad (45)$$

We insert the ansatz (44) in Eq. (26) yielding

$$\Psi_s = 2i\eta_s \operatorname{sech}[2\eta_s(\bar{v} - v_s)t] e^{-i[-p_s(\bar{v} - v_s)t + \Phi_s + (K\bar{v} - \alpha_s)t]}. \quad (46)$$

The fixed points of the phase portrait correspond to the time-independent Ψ , i.e. $\bar{v} = v_s$.

Using Eqs. (45), we obtain two fixed points

$$\operatorname{Re}\Psi_s^\pm = \pm 2\eta_s, \quad \operatorname{Im}\Psi_s^\pm = 0. \quad (47)$$

The \pm signs refer to the two cases in Eqs. (45).

Combining Eqs. (10) and (12) with Eq. (45), α_s can be eliminated and we are left with two equations

$$v_s = 2p_s \pm \frac{a\pi^2}{8\eta_s^2} \operatorname{sech}A_s \tanh A_s, \quad (48)$$

$$-(K - p_s)v_s = p_s^2 - 4\eta_s^2 - \delta \pm \frac{a\pi}{2\eta_s} A_s \operatorname{sech}A_s \tanh A_s, \quad (49)$$

where $A_s = \pi(K - p_s)/(4\eta_s)$. For either sign, the system (48)-(49) has a single root $v_s = 2p_s$, $p_s = K$ and $\eta_s = \frac{1}{2}\sqrt{K^2 - \delta}$. Therefore, there are two fixed points on the real axis, located at $\text{Re}\Psi = \pm\sqrt{K^2 - \delta}$.

For the set of parameters of Fig. 2 there are a stable and an unstable fixed point close to +1 and -1, respectively. The stability of the fixed points is determined by solving the collective coordinates equations numerically with the initial conditions very close to the above values, e.g., $\eta_0 = \eta_s + 10^{-8}$, $q_0 = 0$, $p_0 = p_s$, $\Phi_0 = \Phi_s^\pm = \pm\pi/2$. In the unstable case ($\Phi_0 = -\pi/2$), the numerical solution exhibits oscillations of the amplitude and phase, whereas the velocity of the soliton remains constant. This solution is represented by the separatrix in Fig. 2. A trivial stable fixed point is located at the origin; its stability is established by numerical solutions of the collective coordinates equations with η_s close to zero.

-
- [1] D. J. Kaup and A. C. Newell, Proc. R. Soc. London A **361**, 413 (1978), Phys. Rev. B **18**, 5162 (1978).
 - [2] P.S. Lomdahl and M.R. Samuelson, Phys. Rev. A **34**, 664 (1986).
 - [3] A.W. Snyder and J.D. Love, *Optical Waveguide Theory*, Chapman and Hall (London, 1983).
 - [4] B.A. Malomed, Phys. Rev. E **51**, R864 (1995).
 - [5] G. Cohen, Phys. Rev. E **61**, 874 (2000).
 - [6] K. Nozaki, N. Bekki, Physica D **21**, 381 (1986).
 - [7] I. V. Barashenkov and Y. S. Smirnov, Phys. Rev. E **54**, 5707 (1996).
 - [8] I. V. Barashenkov and E. V. Zemlyanaya, Physica D **132**, 363 (1999).
 - [9] V. M. Vyas, T. S. Raju, C. N. Kumar, and P. K. Panigrahi, J. Phys. A **39**, 9151 (2006).
 - [10] F. G. Mertens, N. R. Quintero and A. R. Bishop, Phys. Rev. E **81**, 016608 (2010).
 - [11] U. Peschel, O. Egorov, and F. Lederer, Opt. Lett. **15**, 1909 (2004).
 - [12] A. Gorbach, S. Denisov, and S. Flach, Opt. Lett. **31**, 1702 (2006).
 - [13] D. Poletti, E. A. Ostrovskaya, T. J. Alexander, B. Li, Y. S. Kivshar, Physica D **38**, 1338 (2009).
 - [14] M. Rietmann, R. Carretero-González, and R. Chacón, Phys. Rev. A **83**, 053617 (2011).
 - [15] M. Salerno and Y. Zolotaryuk, Phys. Rev. E **65**, 056603 (2003).

- [16] L. Morales-Molina, N. R. Quintero, F. G. Mertens, and A. Sánchez, Phys. Rev. Lett. **91**, 234102 (2003).
- [17] A. V. Ustinov, C. Coqui, A. Kemp, Y. Zolotaryuk, and M. Salerno, Phys. Rev. Lett. **93**, 087001 (2004).
- [18] L. Morales-Molina, F.G. Mertens, and A. Sánchez, Phys. Rev. E **72**, 016612 (2005).
- [19] P. Müller, F.G. Mertens, and A.R. Bishop, Phys. Rev. E **79**, 016207 (2009).
- [20] R. Scharf and A. R. Bishop, Phys. Rev. E **47**, 1375 (1993).
- [21] N. G. Vakhitov and A. A. Kolokolov, Radiophys. Quantum Electron. **16**, 783 (1975).
- [22] M. I. Weinstein, Comm. Pure Appl. Math. **39**, 51 (1986).
- [23] Y. Sivan, G. Fibich, B. Ilan, and M. I. Weinstein, Phys Rev E **78**, 046602 (2008).
- [24] N. Akhmediev, A. Ankiewicz, R. Grimshaw, Phys Rev E **59**, 6088 (1999).
- [25] M. M. Bogdan, A. S. Kovalev, and A. M. Kosevich, Sov. J. Low Temp. Phys. **15**, 288 (1989)
- [26] D.E. Pelinovsky, Y. S. Kivshar, and V.V. Afanasjev, Phys. Rev. E **54**, 2015 (1996)
- [27] I. V. Barashenkov, Phys. Rev. Lett. **77**, 1193 (1996).
- [28] I. V. Barashenkov and E. Yu. Panova, Physica D **69**, 114 (1993)
- [29] I. V. Barashenkov, E. V. Zemlyanaya, and M. Bär, Phys. Rev. E **64**, 016603 (2001).
- [30] Y. Kivshar and B. Malomed, Rev. Mod. Phys. **61**, 763 (1989).
- [31] W. L. Kath, Methods and Appl. of Analysis **4**, 141 (1997).
- [32] N. R. Quintero, F. G. Mertens and A. R. Bishop, Phys. Rev. E **82**, 016606 (2010).
- [33] I. V. Barashenkov, Y. S. Smirnov and N. V. Alexeeva, Phys. Rev. E **57**, 2350 (1998).
- [34] I. V. Barashenkov, T. Zhanlav, and M. M. Bogdan, in “ Nonlinear World. IV International Workshop on Nonlinear and Turbulent Processes in Physics”. Editors: V. G. Bar’yakhtar et al. (World Scientific, Singapore,1990), pp. 3-9.
- [35] P. Hänggi and R. Bartussek, in *Nonlinear Physics of Complex Systems-Current Status and Future Trends*, edited by J. Parisi et al., Lecture Notes in Physics Vol. **746** (Springer, Berlin, 1996), p. 476.
- [36] R. D. Astumian and P. Hänggi, Phys. Today **55** (11), 33 (2002).
- [37] P. Hänggi, F. Marchesoni and F. Nori, Ann. Phys. (Leipzig) **14**, 51 (2005).
- [38] F. Jülicher, A. Ajdari, and J. Prost, Rev. Mod. Phys. **69**, 1269 (1997).
- [39] P. Reimann, Phys. Rep. **361**, 57 (2002).
- [40] *Ratchets and Brownian Motors: Basics, Experiments and Applications*, edited by H. Linke

- [special issue of Appl. Phys. A: Mater. Sci. Process. **75**, 2 (2002).
- [41] I. Zapata, R. Bartussek, F. Sols and P. Hänggi, Phys. Rev. Lett. **77**, 2292 (1996).
- [42] F. Marchesoni, Phys. Rev. Lett. **77**, 2364 (1996).
- [43] F. Falo, P. J. Martínez, J. J. Mazo and S. Cilla, Europhys. Lett. **45**, 700 (1999).
- [44] E. Trías, J. J. Mazo, F. Falo, and T. P. Orlando, Phys. Rev. E **61**, 2257 (2000).
- [45] M. Salerno and N. R. Quintero, Phys. Rev. E, **65** 025602(R) (2002).
- [46] G. Costantini, F. Marchesoni and M. Borromeo, Phys. Rev. E **65**, 051103 (2002).
- [47] A. V. Gorbach, S. Denisov, and S. Flach, Chaos **16**, 023125 (2006).
- [48] S. Flach, Y. Zolotaryuk, A. E. Miroschnichenko, and M. F. Fistul, Phys. Rev. Lett. **88**, 184101 (2002).
- [49] L. Morales-Molina, N. R. Quintero, A. Sánchez and F. G. Mertens, Chaos **16**, 013117 (2006).